# Reynolds Stress Measurements for Investigation of Nonlinear Processes of Turbulence in the Large Mirror Device and in the Large Mirror Device-Upgrade

Yoshihiko NAGASHIMA, Sanae-I. ITOH[1], Kimitaka ITOH[2], Akihide FUJISAWA[2],
Shigeru INAGAKI[1], Yoshinobu KAWAI[1], Shunjiro SHINOHARA[1], Masayuki FUKAO[3],
Takuma YAMADA, Kenichiro TERASAKA[1], Takashi MARUTA[1], Kunihiro KAMATAK[1],
Hiroyuki ARAKAWA[1], Masatoshi YAGI[1], Naohiro KASUYA[2], George R. TYNAN[4],
Patrick H. DIAMOND[4], and Yuichi Takase

*The University of Tokyo, Kashiwa, Chiba 277-8561, Japan*
[1] *Kyushu University, Kasuga, Fukuoka 816-8580, Japan*
[2] *National Institute for Fusion Science, Toki, Gifu 509-5292, Japan*
[3] *Myojocho, Uji, Kyoto 611-0014, Japan*
[4] *University of California San Diego, La Jolla, CA 92093, USA*

Based on success of low-frequency zonal potential measurement ($\sim$400 Hz) in the large mirror device [Y. Nagashima JPSJ **77** 114501 (2008)], a multi-channel Reynolds stress probe system has been developed in the large mirror device-upgrade. The system can simultaneously detect fluctuation Reynolds stress at poloidally different 8 locations. Preliminary results from the system demonstrate that poloidally symmetric potential oscillations exist in a frequency range of 200–600 Hz.

Keywords: zonal flow, Reynolds stress, linear plasma device

## 1. Introduction

Understanding of turbulence and transport in self-regulated plasma structure is one of the most important research themes in plasma physics and nuclear fusion research. The drift wave turbulence is considered to dominate in magnetically confined non-uniform plasmas [1]. Recent progress of turbulence study shows that secondary instabilities driven by nonlinearity of the drift wave turbulence may play important roles in self regulation of turbulence [2]. Therefore, observation of self-regulation in turbulent fluctuations (i.e., nonlinear energy transfer among various fluctuations) is a crucial task in turbulence research. In order to investigate the nonlinear energy transfer between drift-wave fluctuations and the secondary instabilities, it is necessary to evaluate off-diagonal terms in momentum balance equations (i.e., the Reynolds stress in the poloidal plane). In particular, the zonal flow and its drive force are precisely defined as poloidally averaged parameters. In the large mirror device (LMD) [3], we measured the local Reynolds stress as well as the zonal potential [4]. In the next stage, we have developed a multi-channel Reynolds stress probe in the large mirror device-upgrade (LMD-U) [5]. In this manuscript, we introduce results from Reynolds stress measurement in linear devices of Kyushu University.

First, we briefly describe results from the large mirror device (LMD). Next, experimental apparatus of a new probe system in the large mirror device-upgrade (LMD-U) is introduced. Finally, we present preliminary results from the probe system in experiments of the spectral transition.

## 2. Summary of the Reynolds Stress Measurement in the LMD

In LMD, secondary instabilities of the drift-wave spectrum have been investigated intensively [4, 6, 7]. A qualitative transition of fluctuation spectrum occurs from combination of coherent spectral peaks to a signature of broadband spectrum due to reducing filling Ar gas pressure $P_{Ar}$ under the fixed magnetic field $B$ of 0.12 T [8]. Previous researches on the transition of fluctuations have been studied in basic plasma experiments in detail, and relationships between the transition and appearance of the low-frequency fluctuations were presented [9, 10]. The co-existence of low-frequency zonal potential ($\sim$400 Hz) and the drift-wave spectrum (7–8 kHz) is observed under the discharge conditions that $P_{Ar}$ $\sim$3.5 mTorr, RF input power is 2 kW, and $B$=0.12 T. The case of $P_{Ar}$ $\sim$3.5 mTorr is the boundary condition of the transition. Nonlinear couplings between the Reynolds stress of the drift-wave spectrum and the zonal potential are successfully detected by a Reynolds stress probe.

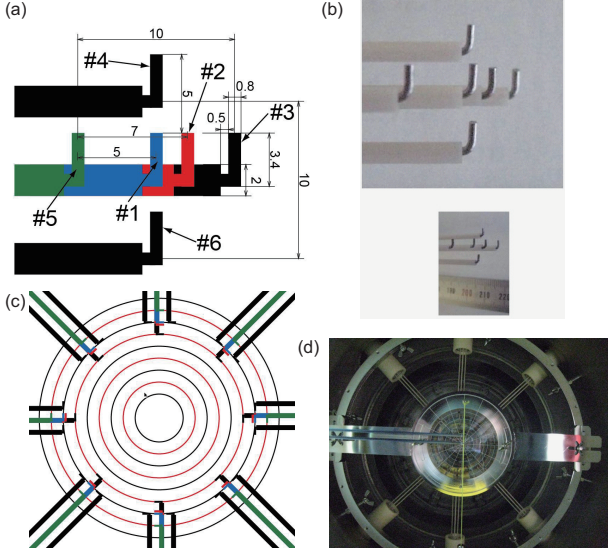*author's e-mail: nagashima@k.u-tokyo.ac.jp*

Fig. 1 (a, c) Schematic views and (b, d) photographs of the multi-channel Reynolds stress probe (MCRSP) system. (a) Enlarged view of the probe head drawing, and (b) photograph of the manufactured probe head. The scale unit is mm. (c) Arrangement of 8 probes at the radial location $r=40$ mm, and (d) calibration scene of the arrangement of the MCRSP system.



Fig. 2 Transition of spectrum during the discharge. (a)Time evolution of the floating potential at $r=4$ cm. Fluctuation spectra before (b) or after (c) the transition.

## 3. Experimental Apparatus in the LMD-U

Based on the success of the Reynolds stress measurement in LMD shown in section 2, a new probe system, multi-channel Reynolds stress probe (MCRSP) system, has been developed in LMD-U, where the nonlinear dynamics of fluctuations have been investigated in detail [11, 12]. A purpose of the system is to measure poloidal variations of the Reynolds stress for investigating the energy transfer among fluctuations with finite poloidal wave numbers. In addition, the system could observe temporal behaviors of poloidal averaged zonal flow and Reynolds stress.

The MCRSP system is located 125 cm away from the end of the vessel (source side). The MCRSP has 8 probes, and each probe head houses six tungsten electrodes which covers simultaneous measurement at different six locations on the poloidal cross-section. The cylindrical electrodes with a diameter of 0.8 mm are bent at tips of the electrodes, as shown in Figs. 1(a) and 1(b). In this experiment, we present observation of the floating potential fluctuation ($\tilde{\Phi}_{\rm f}$). Neglecting the temperature fluctuation, we assume that $\tilde{\Phi}_{\rm f}$ is corresponding to the electrostatic potential fluctuation. The electrodes #3-6 are used mainly for measuring the fluctuation Reynolds stress per mass density (RS). The poloidal and radial distances among the electrodes are 10 mm. The poloidal electric field fluctuation $\tilde{E}_\theta$ and poloidal wave number $k_\theta$ are derived from the electrodes #4 and #6, and the radial elec-
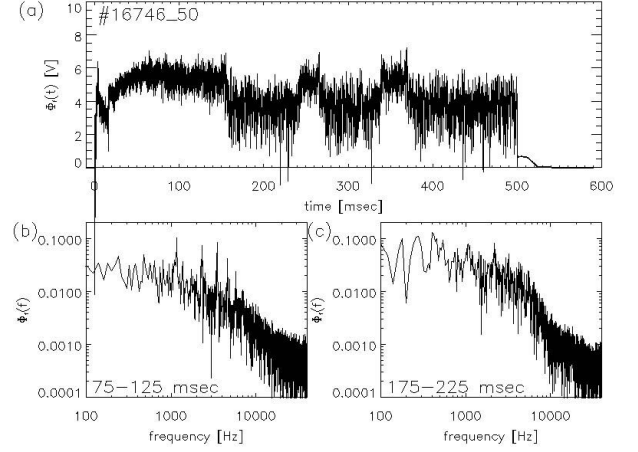
tric field fluctuation $\tilde{E}_r$ and radial wave number $k_r$ are measured by the electrodes #3 and #5. Then we obtain the fluctuation Reynolds stress per mass density $-\langle \tilde{v}_r \tilde{v}_\theta \rangle = \langle \tilde{E}_\theta \tilde{E}_r \rangle$. The electrodes #1 and #2 are available for various purposes. We can check effects of spatial aliasing on fluctuation measurements by use of the electrodes #1-2.

Each probe can move radially, therefore, it is possible to measure poloidal structures of fluctuations at arbitrary radial locations. Figures 1(c) and 1(d) show an arrangement of the 8 probes at the radial location $r=4$ cm. A schematic view of the arrangement is seen in Fig. 1(c), however, the real position of the 8 probes is not the same as the view. Therefore, we calibrated the arrangement by use of polar tick marks printed on a circular transparent board. The center of the transparent board should be set to be in the plasma center. Plasmas in LMD-U are produced in a quartz tube with a length of 40 cm, and we let the laser light through two 0.1 cm holes located at the both ends of the tube. Then, the center of the transparent board is arranged to hit the laser. The laser light also hits the tip of the 2D probe electrode that is located at the plasma center. The 2D probe system detected that our plasmas have circular profiles with poloidal symmetry [13], and this method for identifying the plasma center is valid. The tick marks are adjusted horizontally and vertically by a plumb bob, as shown a yellow vertical line in Fig. 1(d).

## 4. Preliminary results from the MCRSP
### 4.1 Transition of spectrum during discharge

A qualitative transition of spectrum is also found in LMD-U [14, 15]. A boundary condition of the tran-

sition is that $P_{Ar}$ is 3.6-3.9 mTorr and $B$ is fixed at 0.09 T. The transition in LMD-U occurs much faster than that in LMD. The reflected RF power changes just after the transition, and returns gradually to the power level of discharges without the transition (less than 10% of the forward RF power). Figure 2(a) demonstrates the transition during a discharge. The DC floating potential decreases at about 0.15 s, and the first back transition can be seen at about 0.24 s. Two distinctive features of spectrum are found. One is a qualitative change of the spectrum. The spectrum in the beginning of the discharge looks like a combination of coherent spectral peaks in the frequency range of 1–10 kHz as shown in Fig. 2(b). After the transition, the spectrum tends to be closed to broadband one in Fig. 2(c). The other is a behavior of low frequency fluctuations (<1 kHz). The low frequency components increase after the transition. If nonlinear couplings between the low (<1 kHz) and high (1–10 kHz) frequency components occur, it is natural that the bandwidth of the spectrum broadens. Here, we abbreviate the interval before or after the transition as phase **B** or phase **A**, respectively. We use the word "the transition" in the case that the transition occurs from the phase **B** to the phase **A**, and the inverse transition is called "the back transition" in this manuscript.

## 4.2 Arrangement of the probes in the poloidal plane

We calibrated the arrangement of the 8 probes at the same radial location. Based on the observation, here we check the validity of the calibration by mean of polar plots (plot radii or angles are corresponding to potential intensities or probe location angle, respectively) of the stationary $\Phi_f$ which reveal difference of the center location of between plasmas and the arrangement [13].

First, Figure 3(a) shows radial profiles of the stationary floating potential $\overline{\Phi}_f$. The profiles were measured by shot-to-shot radial scans of one probe in the MCRSP system. The $\Phi_f$ after the transition becomes more negative than that before the transition inside the plasma ($r$ <5 cm). Figure 3(b) shows profiles of the amplitude of the floating potential fluctuation in the frequency range higher than 1 kHz $|\tilde{\Phi}_{f,>1\,kHz}|$. The $|\tilde{\Phi}_{f,>1\,kHz}|$ increases after the transition at the radial location $r$ >3 cm. Next, Figure 3(c) shows polar plots of the $\overline{\Phi}_f$ at $r$=4 cm after the transition. Black data indicates plots at the electrodes #1, 2, 4, 6, blue plots are measured at #5, and red plots are the data at #3, respectively. The profile of the $\overline{\Phi}_f$ in Fig. 3(a) shows a positive gradient at $r$=4 cm, and the relationship among black, blue and red plots corresponds to the positive gradient of the $\overline{\Phi}_f$ profile. Considering the variance of the $\overline{\Phi}_f$'s at the same radial locations,
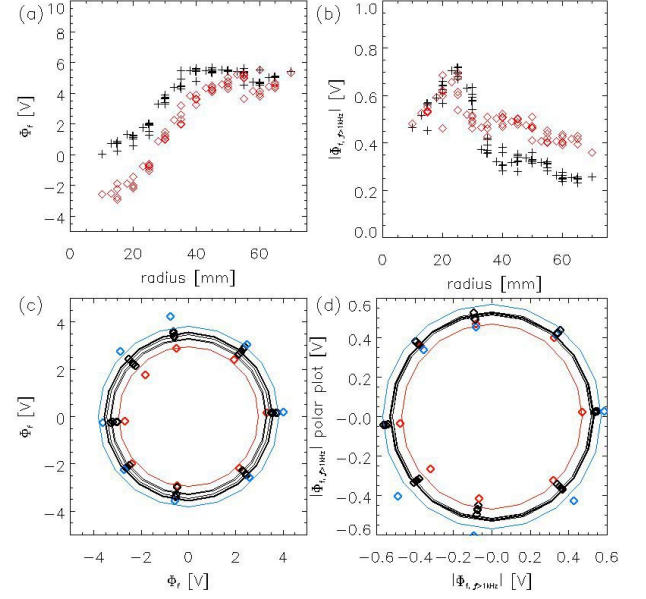


Fig. 3 (a, b) Radial profiles of the floating potential. Profiles of (a) stationary component and (b) fluctuation ($f$ >1 kHz) component. In (a, b), plots in black or red mean profiles before or after the transition. (c, d) Polar plots of the floating potential at $r$=4 cm. Plots of (c) stationary component and (d) fluctuation component. Diamond plots or solid lines indicate measurements by each probe or poloidal averaged values at the same radial locations, respectively. Plots in black indicate data obtained at the electrode#1,2,4,6. Points in blue or red are measured at the electrode #3 or #5, respectively.

discrepancy of the center position between the plasmas and arrangement is roughly ~0.5 cm. In contrast to this, the profile of the $|\tilde{\Phi}_{f,>1\,kHz}|$ in Fig. 3(b) does not show a clear gradient at $r$=4 cm, therefore, polar plots of the $|\tilde{\Phi}_{f,>1\,kHz}|$ in Fig. 3(d) could not discriminate blue and red plots from black plots in terms of the gradient.

## 4.3 Low-frequency potential oscillations and the Reynolds stress

The zonal potential is observed in LMD discharges where the transition occurs. Existence of the low-frequency zonal potential as well as the Reynolds stress are also examined in LMD-U. The zonal potential is related to the Reynolds stress through the vorticity equation $\partial_t \Delta\phi/B = \partial_{rr}\langle E_\theta E_r\rangle/B^2 - \mu\Delta\phi/B$. Therefore, the relationship between the zonal potential and the Reynolds stress can test the causality in the drift wave-zonal flow system. Figure 4 shows spatio-temporal structures of fluctuations in the frequency range of 200–600 Hz. The aliasing in the poloidal direction does not occur. Poloidally symmetric potential oscillations are dominant in Fig. 4(a).
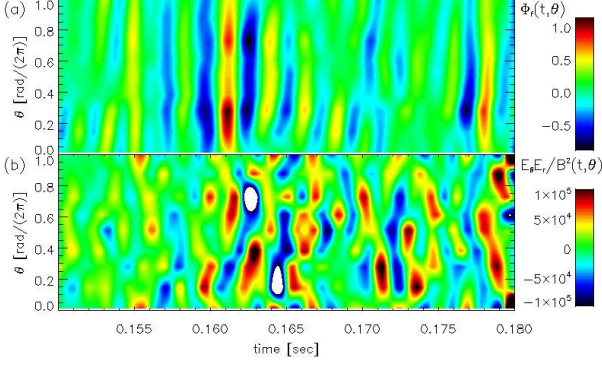
Fig. 4 Temporal behaviors of fluctuations in the frequency range of 200–600 Hz at $r=4$ cm. (a) $\Phi_f(\theta, t)$, and (b) $E_\theta E_r / B^2(\theta, t)$. In calculating the Reynolds stress, the electric field fluctuations are selected in the frequency range of 1–40 kHz. Poloidal profiles are measured by the 8 probes, and void points are interpolated in the contour plots.

However, the poloidal correlation of the oscillations are transiently small, and fluctuations with $m \leq 1$ may be sometimes seen. Fluctuations in the frequency range of 200–600 Hz looks like mixture modes in which the $m=0$ mode is dominant. Figure 4(b) demonstrates that the amplitude of the Reynolds stress oscillation significantly has variation in the poloidal direction.

In reality, to investigate the relationship between the zonal potential and the Reynolds stress, the ensemble average of the vorticity equation performed in the poloidal direction should be considered. We investigated relationship between the transition and the waveforms including poloidally averaged ones. Figure 5 shows waveforms of fluctuations in the frequency range of 200–600 Hz. The contour maps in Figs. 5(a) and 5(c) are the transient behaviors of the poloidal profiles. The waveforms in Figs. 5(b) and 5(d) are averaged poloidally. The transition occurs back and forth, and temporal behaviors of the waveforms are well correlated with the transition phase. All of the fluctuation amplitudes in the phase **A** increase clearly relative to those in the phase **B**.

Our main interest is the correlation of the low-frequency $\langle\Phi_f\rangle(t)$ with the $\langle E_\theta E_r / B^2\rangle\langle\Phi_f\rangle(t)$. The amplitude of the cross-product of them in Fig.5(e) (black) also increases after the transition. The red line in Fig.5(e) is the 10 ms temporal average of the cross-product, and supports the increase. It should be noted that signs of the $\langle E_\theta E_r / B^2\rangle\langle\Phi_f\rangle(t)$ are not unique transiently. The positive sign indicates that the $\langle\Phi_f\rangle(t)$ and the $\langle E_\theta E_r / B^2\rangle\langle\Phi_f\rangle(t)$ are in phase, and the negative sign means the opposite. The positive sign of the $\langle E_\theta E_r / B^2\rangle\langle\Phi_f\rangle(t)$ tends to be seen just after the transition, and the negative one can be seen just after the back transition. Further studies are necessary to conclude the tendency of the appearance
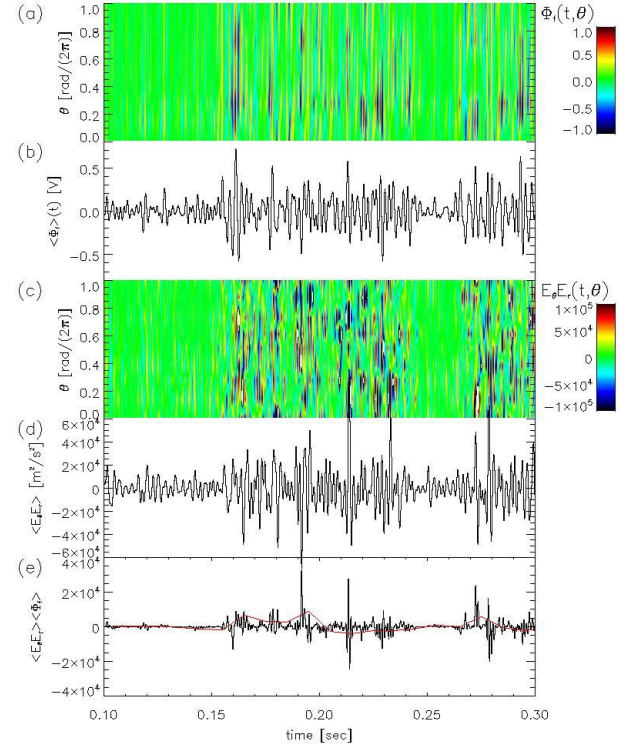


Fig. 5 Relationships between the transition and the waveforms in the frequency range of 200–600 Hz at $r=4$ cm. (a) $\Phi_f(\theta, t)$, (b) $\langle\Phi_f\rangle(t)$, (c) Reynolds stress $E_\theta E_r / B^2(\theta, t)$, (d) $\langle E_\theta E_r / B^2\rangle(t)$, and (e) $\langle E_\theta E_r / B^2\rangle\langle\Phi_f\rangle(t)$. The black line in (e) is a raw plot of the $\langle E_\theta E_r / B^2\rangle\langle\Phi_f\rangle(t)$, and the red line is given by multiplying the 10 ms temporal average of the black line by 16.

of the positive and negative signs.

## 5. Summary and Future Direction

In summary, to investigate nonlinear dynamics of fluctuations poloidally and radially in detail, the multi-channel Reynolds stress probe system has been installed in the large mirror device-upgrade. The system is successfully arranged in the poloidal direction at the same radial location, and validity of the arrangement is confirmed by a test using the experimental profile data. We applied the system to experiments of the discharge in which the spectral transition occurs. The preliminary results from the system demonstrates that the low frequency (200–600 Hz) floating potential fluctuations with $m=0$ are observed. In addition, fluctuations with $m \leq 1$ at the same frequency as the $m=0$ modes may be observed transiently. Oscillation of the poloidally averaged Reynolds stress is correlated with the $m=0$ modes. and The correlation after the transition becomes larger than that before the transition.

To identify the nonlinear energy transfer between the zonal flow and the Reynolds stress gradient in

terms of the poloidal average, it is necessary to measure poloidal profiles of the fluctuations at two different radial locations. Therefore, installation of the additional 8 probes as well as diagnostics for the direct ion flow such as the Mach probe is under consideration in the future.

[1] W. Horton, Rev. Mod. Phys. **71**, 735 (1999).
[2] P.H. Diamond, S.-I. Itoh, K. Itoh, and T.S. Hahm, Plasma Phys. Control. Fusion **47**, R35 (2005).
[3] Y. Saitou, et al., Phys. Plasmas **14**, 072301 (2007).
[4] Y. Nagashima, et al., J. Phys. Soc. Jpn. **77**, 114501 (2008).
[5] S. Shinohara, et al., 28th Int. Conf. on Phenomena in Ionized Gases, Prague, Czech Republic, 1P04-08, 345-357 (Institute of Plasma Physics, AS CR, Prague, 2007).
[6] Y. Nagashima, et al., Proc. 35th EPS on Plasma Physics, P-5.158 (2008).
[7] Y. Nagashima, et al., Plasmas Fusion Res. **3**, 056 (2008).
[8] Y. Nagashima, et al., Bulletin of 48th DPP, APS, JP1.00087 (2006).
[9] T. Klinger, A. Latten, A. Piel, G. Bonhomme, T. Pierre, and T. Dudok de Wit, Phys. Rev. Lett. **79**, 3913 (1997).
[10] M. Burin, G. R. Tynan, G. Antar, N. Crocker, and C. Holland, Phys. Plasmas **12**, 052320 (2005).
[11] T. Yamada, et al., Plasma Fusion Res. **2**, 051 (2007).
[12] T. Yamada, et al., Nat. Phys. **4**, 721 (2008).
[13] T. Yamada, et al., Rev. Sci. Instrum. **78**, 123501 (2007).
[14] K. Terasaka, et al., Plasma Fusion Res. **2**, 031 (2007).
[15] S. Inagaki, et al., Proc. 35th EPS on Plasma Physics, P-4.044 (2008).